solubility increases greatly; a similar effect is observed in the presence of $CO_3^{2-}$. In the presence of both of these anions, that is, in synthetic Mono Lake water either with or without added $Fe^{3+}$, the solubility of plutonium is virtually 100 percent, as in actual Mono Lake water. These results suggest that the solubility of plutonium in Mono Lake water is the result of complexation by both $CO_3^{2-}$ and $F^-$. The overall stability constants of $PuF^{3+}$ and $PuF_2^{2+}$ are approximately $10^8$ and $10^{14}$, respectively (*7*), values that are not large enough to prevent hydrolysis at *p*H 10 (*8*). Although no reliable values exist for complexes of Pu(IV) and $CO_3^{2-}$ (*7*), they are unquestionably large. Our data do not allow a conclusion as to whether mixed-ligand complexes or merely a mixture of single-ligand complexes are present.

Although $CO_3^{2-}$ and $F^-$ are responsible for the solubility of plutonium, the oxidation-state distribution of plutonium appears to be determined by the dissolved iron. The solubility of plutonium in synthetic Mono Lake water containing no added $Fe^{3+}$ is similar to that of the actual water, but the oxidation-state distribution differs greatly in that there is a much larger percentage of Pu(III). In the presence of added $Fe^{3+}$ (as $FeCl_3$), however, both the solubility and the oxidation-state distribution of plutonium in the synthetic water are similar to those in actual Mono Lake water. This finding is consistent with our earlier conclusion (*6*) that ionic species, rather than dissolved oxygen, determine the oxidation-state distribution of actinides in solution. Moreover, the solubility of plutonium in synthetic Mono Lake water without added $FeCl_3$, despite the preponderance of Pu(III), is consistent with results in other waters (*6*) and suggests that Pu(III) is also stabilized by complexing.

This suggestion was further confirmed by the behavior of Am(III), a close analog of Pu(III) except for its existence in natural waters solely in the trivalent state, which also was soluble in Mono Lake water over the 30-day period of study. Reliable stability constants for $CO_3^{2-}$ and $F^-$ complexes of Pu(III) are lacking (*7*), but they do exist for Am(III). The overall stability constants of $AmCO_3^+$ and $Am(CO_3)_2^-$ have been reported as $6.5 \times 10^5$ and $5.2 \times 10^9$, respectively (*9*), and for $AmF^{2+}$ as 310 (*10*), all at 1*M* ionic strength and 25°C. On the basis of stability constants and higher ligand concentration, the $CO_3^{2-}$ complexes of Pu(III) would predominate strongly over the $F^-$ complexes; a similar preponderance of Pu(IV)–$CO_3^{2-}$ species would be expected if one assumes the same relative order of stability for complexes of the tetravalent ion.

JESS M. CLEVELAND
TERRY F. REES
KENNETH L. NASH
*U.S. Geological Survey,*
*Denver, Colorado 80225*

### References and Notes

1. H. J. Simpson, R. M. Trier, C. R. Olsen, D. E. Hammond, A. Ege, L. Miller, J. M. Melack, *Science* **207**, 1071 (1980).
2. H. J. Simpson, R. M. Trier, J. R. Toggweiler, G. Mathieu, B. L. Deck, C. R. Olsen, D. E. Hammond, C. Fuller, T. L. Ku, *ibid.* **216**, 512 (1982).
3. R. F. Anderson, M. P. Bacon, P. G. Brewer, *ibid.*, p. 514.
4. The use of trade names is for descriptive purposes only and does not constitute endorsement by the U.S. Geological Survey.
5. E. A. Bondietti and S. A. Reynolds, in *Proceedings of the Actinide-Sediment Reactions Working Meeting, Seattle, Washington, February 10 and 11, 1976*, L. L. Ames, Ed. (Department of Energy Report BNWL-2117, Battelle Pacific Northwest Laboratory, Richland, Wash., 1976), pp. 505–530.
6. J. M. Cleveland, T. F. Rees, K. L. Nash, *Nucl. Technol.* **62**, 298 (1983).
7. J. M. Cleveland, in *Chemical Modeling in Aqueous Systems*, E. A. Jenne, Ed. (Symposium Series 93, American Chemical Society, Washington, D.C., 1979), pp. 321–338.
8. K. L. Nash and J. M. Cleveland, in preparation.
9. R. Lundquist, *Acta Chem. Scand. Ser. A* **36**, 741 (1982).
10. G. R. Choppin and P. J. Unrein, in *Transuranium Elements*, W. Mueller and R. Lindner, Eds. (North-Holland, Amsterdam, 1976), pp. 97–107.
11. We thank V. Pearce for supplying the Mono Lake water used in this study. This water was analyzed by the U.S. Geological Survey National Water Quality Laboratory in Denver.

13 June 1983; accepted 8 September 1983

## Van der Waals Surfaces in Molecular Modeling: Implementation with Real-Time Computer Graphics

Abstract. *A method is described for generating van der Waals molecular surfaces with a real-time interactive calligraphic color display system. These surfaces maintain their proper representation during bond rotation and global transformations, and an interior atom removal method yields a comprehensible picture of the molecular surface for large molecules. Both algorithms are faster than previous methods. This combination provides a powerful tool for real-time interactive molecular modeling.*

Molecular modeling with interactive color computer graphics in real time is a powerful method for studying the structures of molecules and their interactions (*1–3*). Computer-generated skeletal models maintain a consistent representation during manipulations such as bond rotations and global transformations but have the disadvantage that they give no indication of the physical space occupied by the atoms. We describe here a method for representing molecular surfaces that, unlike previous methods, is suitable for real-time interaction and manipulation.

With raster graphics atomic surfaces may be represented by shaded colored spheres. The displayed molecular surface is constructed by removing hidden surfaces of intersecting and overlapping spheres (*4, 5*) and shows a molecule in a given orientation and conformation. To view the molecule from another angle or in another conformation, one must generate an entirely new surface. Because hidden surface elimination may take several minutes on present equipment, this representation is of limited use in real-time molecular modeling. Several methods based on line drawing displays are available for similar static hidden-line representations (*6*). Other methods are based on an original idea by Richards (*7*) in which a "solvent-accessible surface" is traced out by the inward-facing surface of a "solvent sphere" making contact with the van der Waals surface of atoms in the molecule. This was first developed for studies of molecular interactions by using an interactive monochrome display (*8*), and later extended (*9*) for an interactive color display by using dots to represent the exterior solvent-accessible surface and internal cavities. A similar molecular surface may be generated more rapidly by using a "bit" lattice (*10*). Although these surfaces (*8–10*) may be globally manipulated in real time, bond rotation still requires recalculation of the area affected by the change. Therefore, modeling with molecular surfaces of this variety and frequent changes in torsion angles is laborious.

We have developed a method that generates a molecular surface faster than the above method and which has the significant advantage that the space-filling representation is retained during interactive real-time bond rotation. The ability to change the conformation of the molecular surface in real time cannot be overemphasized (*11, 12*).

For each atom surfaced, we generate a set of points distributed uniformly over a sphere whose radius is the van der Waals radius of the atom. Each point is com-

pared against the spheres associated with each connected atom and discarded if it lies inside any other sphere. This conceptually simple algorithm produces a precise representation of the van der Waals surface of a molecule (*13*) and is displayed and manipulated interactively in real time.

These surfaces are well suited for molecules of about 100 atoms or less, but the inclusion of all interior atoms and their surfaces for a large molecule, such as a protein, produces a confusing image. Hence, we invoke another procedure for the removal of interior atoms. We use a bit lattice similar to that described by Pearl and Honegger (*10*) and map the coordinates of each atom onto a discrete three-dimensional Cartesian grid. The extent of an atom is represented by a cube of 3 by 3 by 3 grid points; the center of the cube corresponds to the center of the atom. The distance between adjacent grid points is typically chosen to be 1.6 Å. Grid points that represent atoms are considered occupied and all others unoccupied. To select interior atoms, the grid is searched in each orthogonal direction to determine the surface grid points, defined as those occupied grid points adjacent to unoccupied ones. An atom that has no surface grid points associated with it is defined as an interior atom (*14*). A van der Waals surface is then generated for each selected surface atom to produce the molecular surface.

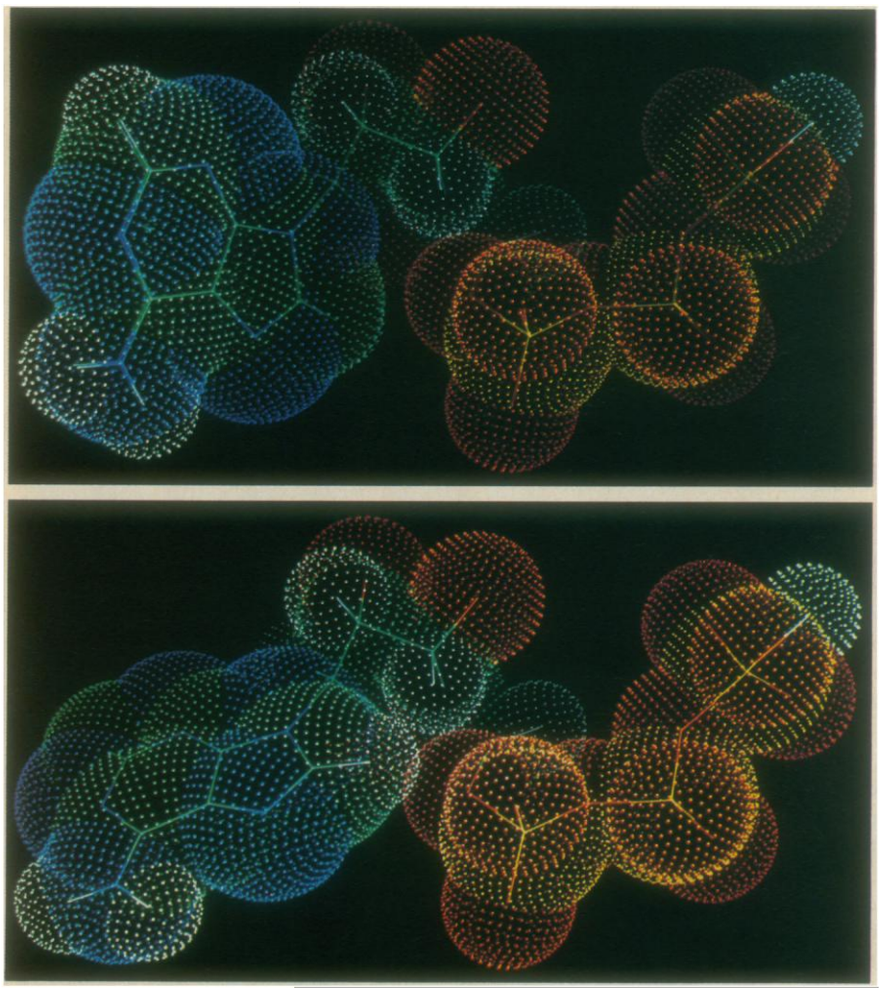

Fig. 1. (top) Van der Waals molecular surface of ATP, shown at a density of 25 dots per square angstrom. The surface is color-coded by atom type: carbon (green), nitrogen (blue), oxygen (red), and hydrogen (white). (bottom) The same surface after real-time rotation about the glycosyl bond.

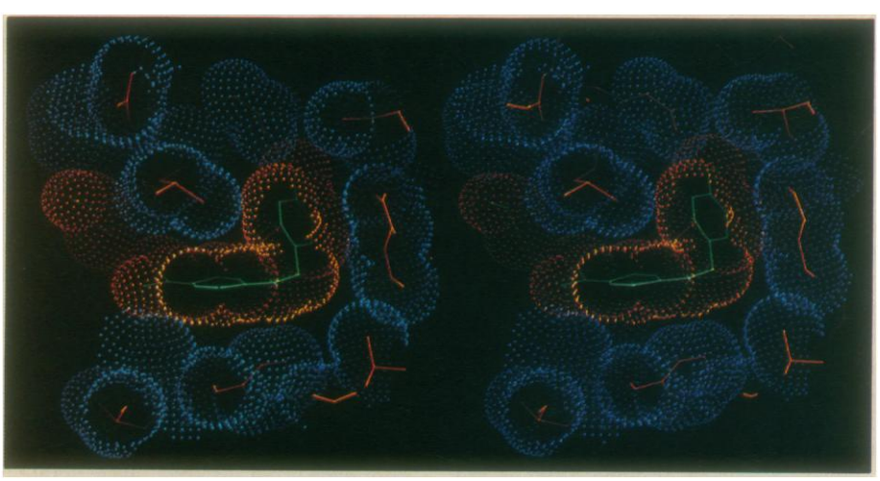

Fig. 2. Stereo view of the van der Waals surface of the noninterior atoms in a section of the active site of dihydrofolate reductase (blue dots), the skeletal model of the residues in the active site (red lines), and the methotrexate molecule and its van der Waals molecular surface (green lines and red dots).

The entire surface of a large molecule is usually not required when modeling interactions with other molecules, such as binding of drugs to receptors. We select a site by searching for atoms in a molecule within a given distance from a defined set of coordinates in the region of interest. Interior atom removal is then invoked and atoms selected both as site and surface atoms can be displayed.

Figure 1 shows the skeletal model and the van der Waals surface of adenosine triphosphate (ATP) (*15*) in two different conformations. The surface dots are color-coded by atom type, and their density is chosen as 25 dots per square angstrom to illustrate the features of the surface. This surface maintains an accurate space-filling representation during bond rotation. It should be emphasized that the bond rotations shown in Fig. 1 were performed in real time without recalculation of the surface.

To illustrate molecular interactions, a section of the active site of dihydrofolate reductase occupied by the antineoplastic drug methotrexate (*16*) is shown in Fig. 2. The skeletal model of the active site residues—those containing atoms within 6 Å of any atom in methotrexate—is shown with red lines. The surfaces of atoms selected as both active site and surface atoms are represented as blue dots; the green lines and red dots represent the methotrexate molecule and its surface, respectively (*17*). To study this interaction in more detail, the conformation of either molecule and its surface can be varied interactively in real time, and global transformations such as scaling, rotation, translation, and sectioning may be performed to optimize

the view. The speed of determining such a binding site, the generation and display of its surface and the surface of its substrate, and the ability to change the conformation of both molecules in real time are significant advantages in drug design. With the methods described in this report, it is possible to examine the steric interaction of many drugs with their receptors efficiently and rapidly. The resultant images are also very beautiful.

PAUL A. BASH
NAGARAJAN PATTABIRAMAN
CONRAD HUANG
THOMAS E. FERRIN
ROBERT LANGRIDGE
*Computer Graphics Laboratory, Department of Pharmaceutical Chemistry, University of California, San Francisco 94143*

### References and Notes

1. R. Langridge, T. E. Ferrin, I. D. Kuntz, M. L. Connolly, *Science* **211**, 661 (1981).
2. J. M. Blaney *et al.*, *J. Med. Chem.* **25**, 785 (1982).
3. P. K. Weiner, R. Langridge, J. M. Blaney, R. Schaefer, P. A. Kollman, *Proc. Natl. Acad. Sci. U.S.A.* **79**, 3754 (1982).
4. T. Porter, *Comput. Graphics* **12**, 282 (1978); R. J. Feldmann, D. H. Bing, B. C. Furie, D. Furie, *Proc. Natl. Acad. Sci. U.S.A.* **75**, 5409 (1978).
5. N. L. Max, *Comput. Graphics* **13**, 165 (1979).
6. G. M. Smith and P. Gund, *J. Chem. Inf. Comput. Sci.* **18**, 207 (1978).
7. F. M. Richards, *Annu. Rev. Biophys. Bioeng.* **6**, 151 (1977); B. Lee and F. M. Richards, *J. Mol. Biol.* **55**, 379 (1971).
8. J. Greer and B. L. Bush, *Proc. Natl. Acad. Sci. U.S.A.* **75**, 303 (1978).
9. M. L. Connolly, *Science* **221**, 709 (1983).
10. L. H. Pearl and A. Honegger, *J. Mol. Graphics* **1**, 9 (1983).
11. This surface generator is now one of the commands (VDW) in MIDAS (Molecular Interactive Display and Simulation), a program for the display and manipulation of molecular models developed by C. Huang, T. E. Ferrin, L. Gallo, and R. Langridge at the Computer Graphics Laboratory, University of California, San Francisco, and used in all the work reported here. All programs were written in C and run with the UNIX time-sharing system (*12*) on a DEC VAX 11/750 by using an Evans & Sutherland Color Picture System 2. The software also runs on a VAX 11/780 under VMS with an Evans & Sutherland Color MultiPicture System, and similar software is under development for an Evans & Sutherland Color Picture System 300.
12. D. M. Ritchie and K. Thompson, *Commun. ACM* **17**, 7 (1974). UNIX is a registered trademark of Bell Laboratories.
13. The algorithm takes 0.03 central processing unit (CPU) seconds per atom at a density of five dots per square angstrom. Generation time is proportional to dot density. The algorithms of Connolly (*9*) and Pearl and Honegger (*10*) require 5 and 0.18 CPU seconds per atom, respectively, on comparable computers.
14. Interior atom removal takes 0.02 CPU seconds per atom.
15. O. Kennard, N. W. Isaacs, W. D. S. Motherwell, J. C. Coppola, D. L. Wampler, A. C. Larson, D. G. Watson, *Proc. R. Soc. London Ser. A* **325**, 401 (1971).
16. D. A. Matthews *et al.*, *J. Biol. Chem.* **253**, 6946 (1978).
17. The entire process of site selection, surface atom selection, and surface generation for dihydrofolate reductase took 30 CPU seconds, and the surface generation of methotrexate took less than 2 CPU seconds.
18. We thank K. Davies, I. D. Kuntz, J. McClarin, and S. J. Oatley for discussions. Supported by NIH grant RR-1081 (R.L.), NIH graduate training grant GM-07379 (P.A.B.), and the University of California. P.A.B. is a graduate student in the Biophysics Graduate Group at the University of California, Berkeley.

6 May 1983; revised 29 June 1983

# Epsilon Carbide: A Low-Temperature Component of Interplanetary Dust Particles

Abstract. *Transmission electron microscope study of a chondritic interplanetary dust particle has revealed the presence of epsilon iron-nickel carbide, a low-temperature carbide previously encountered only in metallurgical studies. In these studies* ϵ*-carbide was synthesized by carburization of iron or nickel grains in a stream of carbon monoxide or carbon monoxide plus hydrogen. Similar carburization of an iron-nickel metal in situ may have produced* ϵ*-carbide during particle heating on atmospheric entry or in solar orbit. Alternatively, the* ϵ*-carbide may be a by-product of Fischer-Tropsch reactions in the solar nebula. Such reactions have been proposed as the mechanism of hydrocarbon formation in the early solar system.*

Interplanetary dust particles (IDP's) collected in the stratosphere have been established as a new family of extraterrestrial materials, of which the subset of particles termed chondritic or C-type (*1*) shows evidence of containing material from the early solar system (*2, 3*). Although transmission electron microscope (TEM) studies of C-type particles have revealed some systematic aspects of their mineralogies and microstructures, many features exhibited by specific particles and by the group as a whole remain enigmatic, and new mineralogical problems have appeared frequently in the course of IDP research. We report here TEM observations of ϵ-carbide from a C-type particle. The presence of this phase in IDP's was recently discovered in both our laboratory and that of D. Brownlee (*4*). This carbide has apparently not been observed previously in extraterrestrial materials, and we believe it represents a significantly new aspect of the mineralogy of chondritic IDP's.

The carbide was identified during a TEM study of particles obtained from the NASA cosmic dust collection. It occurs in a particle (NASA No. U2001B17) approximately 10 μm in size that is intermediate between the chondritic-porous (CP) and chondritic-smooth (CS) morphological types defined by Brownlee *et al.* (*1*). The particle has "typical" C-type mineralogy: predominant grains of essentially pure enstatite in an extremely fine-grained, presumably carbonaceous, matrix containing magnetite and iron sulfide. The TEM preparation procedures entailed crushing the particle between clean glass slides and transferring the fragments to a thin-carbon film on a copper grid (*5*).

The carbide and associated phases were identified by electron diffraction and energy dispersive x-ray spectroscopy (EDS). Single-crystal diffraction patterns were obtained with a focused probe (convergent-beam electron diffraction) as well as by conventional selected-area electron diffraction. Four crystals of ϵ-carbide were identified and occur as distinct 1000- to 2000-Å grains separated from the matrix material. One of the carbide grains has smaller grains of magnetite around its margin. These do not share grain boundaries with the carbide, but were presumably adjacent to it in the matrix prior to crushing. The EDS spectra from the carbide show major iron and minor nickel in an approximate atomic ratio of 8:1 (*6*).

Single-crystal electron diffraction patterns of the carbide are shown in Fig. 1. Subsidiary reflections along the 4.0-Å and 4.3-Å rows are characteristic. The periodicities and angles from these patterns and seven others showed good agreement with the published diffraction data for ϵ-carbide (*7, 8*). Measurements were specifically carried out on successive reciprocal lattice sections obtained on rotation about the 4.0-, 4.3-, and 2.3-Å rows (Fig. 1). The results confirmed that the reciprocal lattice contains only vectors permitted by the ϵ-carbide supercell.

According to Nagakura (*8*), the ϵ-Fe carbide structure is based on a hexagonal close-packed (hcp) sublattice of iron atoms with one-third of the octahedral sites occupied by carbon. Octahedral vacancies are ordered onto every third atomic plane along unit cell direction $a$, producing superlattice reflections along $h00$ and a supercell with $a = \sqrt{3}\ a_{hcp}$.

The diffraction patterns in Fig. 1 are indexed according to this supercell. The appearance of faint forbidden $00l$ ($l$ = odd) reflections is consistent with multiple diffraction effects. There is apparently complete solid solution between ϵ-$Fe_3C$ and ϵ-$Ni_3C$ with little change in overall structure or lattice parameters (*8, 9*). Jack (*7*) reports that the metal/carbon ratio can vary between 2 and 3. This ratio for the present phase is unknown.

Carbides with the epsilon structure have been identified in martensite after low-temperature (~ 200°C) tempering (*7*) and have been synthesized from metal films and powders under CO or CO + $H_2$ gas streams (*8–10*). Conversion of magnetite and iron metal cata-